

**CASE FILE**  
**COPY**

AUG 15 1955

NACA TN 3487

**NATIONAL ADVISORY COMMITTEE  
FOR AERONAUTICS**

**TECHNICAL NOTE 3487**

ACOUSTIC RADIATION FROM TWO-DIMENSIONAL RECTANGULAR  
CUTOUTS IN AERODYNAMIC SURFACES

By K. Krishnamurty

California Institute of Technology

FRANCIS & TAYLOR CHILD  
ENGINEERING LIBRARY



Washington

August 1955

33



## NATIONAL ADVISORY COMMITTEE FOR AERONAUTICS

## TECHNICAL NOTE 3487

## ACOUSTIC RADIATION FROM TWO-DIMENSIONAL RECTANGULAR

## CUTOUTS IN AERODYNAMIC SURFACES

By K. Krishnamurty

## SUMMARY

Subsonic and supersonic flow of air past rectangular cavities cut into a flat surface were studied. The cavities were found to emit a strong acoustic radiation. These acoustic fields were investigated by means of schlieren observation, interferometry, and hot-wire anemometer.

The frequency of the sound, as measured by a hot-wire, at a fixed depth of the gap was found to be inversely proportional to the breadth. No simple relationship was noticed between the Mach number  $M_\infty$  and a nondimensional frequency  $S$  based on the gap breadth and the free-stream velocity.

The intensity of the radiation was conveniently measured by means of an optical interferometer of the Mach-Zehnder type. At a Mach number of 0.8, a unit fringe shift was found to correspond to an intensity level of 160 decibels. Fringe shifts equal to and greater than 1 were observed for the radiations from these cavities, indicating that the acoustic fields were very intense.

## INTRODUCTION

The problem of flow past cavities in solid boundaries embraces a number of phenomena of great practical and fundamental interest. The buffeting of bomb bays and open cockpits is a typical problem of this type. Cavity flow is a special case of the general problem of flow past a bluff body, the essential feature of which is the establishment of a balance between pressure fields in the wake and driving forces of the outside flow. Thus, a study of the energy balance and the force distribution between the outside flow and the flow in the cavity may lead to a better understanding of the general problem.

On such considerations as these, an investigation of aerodynamic cavities in low and high speed flows was undertaken at the Guggenheim Aeronautical Laboratory, California Institute of Technology. The

experiments in high-speed flow showed that an intense, high-frequency acoustic radiation is an essential feature of the problem. Consequently, a study of the acoustic field (involving schlieren observations and frequency and intensity measurements) was undertaken. This report presents the salient features of the study, which was mainly exploratory.

This work was conducted at GALCIT under the sponsorship and with the financial assistance of the National Advisory Committee for Aeronautics. The author is deeply indebted to Dr. Anatol Roshko and Professor H. W. Liepmann for their guidance and interest. Special thanks are due Miss Clara Baum for the preparation of the report and Mr. Johannes de Bruyn, who was of valuable assistance in performing the experiments.

#### SYMBOLS

a	local speed of sound
b	width of cavity
d	depth of cavity
f	frequency
I	intensity
k	Gladstone-Dale constant
l	span of model
M	Mach number
P	maximum amplitude of pressure wave
S	nondimensional frequency of Strouhal number
T	temperature
U	flow velocity
V	relative velocity of wave propagation
x	fringe spacing, distance between two consecutive fringes
$\Delta x$	fringe shift

$\alpha$	constant of proportionality between $f$ and $1/b$
$\delta$	condensation, $\Delta\rho/\rho_e$
$\delta^*$	maximum amplitude of condensation wave
$\lambda$	actual wavelength of acoustic radiation
$\lambda_v$	wavelength in vacuum of monochromatic light used in interferometry
$\rho$	instantaneous local density
$\Delta\rho = \rho - \rho_e$	
$\rho_e$	equilibrium value of local density

## Subscripts:

db	decibel
m	maximum
o	stagnation conditions
ref	reference
w	wedge
l	conditions just ahead of cavity
$\infty$	free-stream conditions

## EXPERIMENTAL EQUIPMENT AND SETUP

## Wind Tunnel

The investigations were made in the GARCIT 4- by 10-inch transonic wind tunnel, which can be continuously operated over a Mach number range of 0.25 to 1.5.

The optical methods used were a conventional Toepler's schlieren system and a Mach-Zehnder interferometer. These were equipped with short-duration light sources. The interferometer source consisted of a spark discharge between magnesium electrodes and an interference filter for the 5,170 Å magnesium line. The effective duration of the flash was of the order of 2 to 3 microseconds.

### Model

Exploratory observations were made with various models. The final measurements used a single model spanning the tunnel to obtain gaps of various breadths, the depth being the same for all of them. Figures 1 and 2 show the general features of construction and installation of the model. It was made in two parts. The bottom part was a flat plate supported in the movable windows of the tunnel, where its angle of attack could be changed easily. Its nose was formed by a  $30^\circ$  wedge. A step 0.1 inch deep was cut in the upper surface of the plate.

The top part of the model was a rectangular plate 0.1 inch thick. This was constrained, by means of two thin rails, to slide over the bottom part behind the step. The movement was provided by a rack and pinion arrangement, which made it possible to vary the breadth of the gap continuously while the tunnel was operating. Another rack carrying a needle indicator recorded the breadth of the gap on a 0.01-inch scale. The gap breadth could be varied from 0 to 2 inches.

The maximum thickness of the model was 0.3 inch. It was not possible to increase the thickness and thus obtain a deeper gap without lowering the subsonic choking Mach number below 0.8.

The top surface and the leading edge of the model were maintained very smooth in order to obtain a laminar boundary layer ahead of the cavity.

### Hot-Wire Setup

A tungsten wire, 0.00015 inch in diameter and  $3/16$  inch long, was carried by two steel needles fixed in a Bakelite plug, which was inserted into a suitable recess cut into the model (fig. 2). The electrical leads were carried out through one of the model supports. The wire was heated by a constant current of 25 milliamperes, its signal being fed into an amplifier with a total gain of approximately 4,000 and a constant frequency response up to 70 kilocycles. The hot-wire was not compensated up to this frequency, but it was found that a signal, sufficiently strong for frequency measurements, could be obtained. The output of the amplifier was examined on an oscilloscope and two wave analyzers, one with a frequency range of 15 to 500 kilocycles and the other with a range of 30 to 16 kilocycles.

### Reynolds Numbers

When the model was set with its upper surface parallel to the free-stream direction, flow with laminar boundary layer ahead of the gap was

obtained (a slight negative angle of attack was found beneficial). The Reynolds number at the gap, based on the distance of its upstream edge from the leading edge of the plate, varied approximately from  $0.75 \times 10^6$  to  $1.1 \times 10^6$  for Mach numbers of 0.45 to 0.8, respectively.

To obtain turbulent boundary layers, a trip wire was attached close to the leading edge of the model. However, for the interferometric studies the tripping of the boundary layer was accomplished simply by setting the model at a suitable positive angle of attack.

#### DESCRIPTION OF PHENOMENA

Schlieren studies and direct frequency measurements showed that two-dimensional rectangular cavities cut into an aerodynamic surface gave rise to acoustic radiation both in subsonic and supersonic flows (figs. 3, 4, and 5). Such radiation had been observed for cavities of varying dimensions and for flows with either laminar or turbulent boundary layers ahead of the cavity. The character of the acoustic field was found to depend upon the type of boundary layer, the gap dimensions, and the free-stream velocity or Mach number.

In all cases, for a given gap at a particular Mach number, the radiated field was weaker with a turbulent boundary layer ahead of the gap than with a laminar layer. For the laminar case the waves were well defined and could be observed very clearly with the spark, while for the turbulent case they appeared weak and diffused.

It was observed in experiments on the variable gap (where the depth was fixed while the breadth was varied) that the minimum breadth at which sound emission was first noticed depended on the Mach number, being smaller for the higher Mach numbers than for the lower ones. No precise measurements of the minimum breadths were made. It was noted, however, that, for the same Mach number, emission in the case of the turbulent layer seemed to commence at a slightly larger breadth than in the laminar case. For instance, for a gap width of 0.1 inch and at a Mach number of 0.75, neither discrete frequencies nor any sound waves were observed in the case of the turbulent boundary layer, contrary to the laminar case.

For breadths smaller than the minimum, the shear layer leaving the upstream edge of the gap bridged across the gap to the downstream edge.

The waves at the minimum breadth for any given Mach number appeared weak and were of the shortest wavelength for that Mach number. Schlieren pictures and interferometric studies showed that, as the breadth was gradually increased, the wavelength correspondingly became larger, while

the intensity increased initially and then decreased gradually. The wavelength of the emitted acoustic field was directly proportional to the breadth of the gap. Figures 3(a) to 3(d) are spark schlieren photographs of the phenomena for increasing gap breadths at a Mach number of 0.815 and with a laminar boundary layer ahead of the gap. The turbulent case is shown in figures 5(a) to 5(c). (The dark projection in the gap in some of these pictures is the hot-wire needle.)

No precise determination was made of the minimum Mach number at which acoustic radiation from a given gap was first detectable. For gap widths greater than 0.3 inch, approximately 0.4 was the minimum Mach number at which discrete frequencies were measured (fig. 6). For these gap sizes waves in the external flow were observed for Mach numbers 0.45 and above. For Mach numbers below 0.4, neither frequencies related to the gap breadths nor waves were noted for any of the gap sizes.

At low Mach numbers, up to 0.65, the radiation was not very directional or strong (figs. 4(a) and 4(b)). As the Mach number increased, the radiation became more and more intense and directional (figs. 4(c) and 4(d)). The radiation pattern for the intense fields could be observed with the schlieren system and continuous-light source. Examples of such continuous-light pictures, showing the directed beams at  $M_\infty = 0.803$  for the laminar case, are given in figures 7(a) and 7(b) for gap breadths of 0.1 and 0.2 inch, respectively. In both cases radiations in three directions are noticeable, the downstream one being the strongest. As the breadth was increased, the upstream radiations became weaker and even at  $b = 0.3$  they were not visible on the continuous schlieren. The directions of the radiation for the cases shown are given in the following table. The direction for each beam is given in degrees, measured from the downstream surface of the flat plate.

Gap, in.	Direction of radiation, deg		
	Upstream	Middle	Downstream
0.1 by 0.1	107.5 to 147	93	77.5 to 72
0.1 by 0.2	106.5 to 160	106.5 to 102	76.5 to 75

Larger gap widths or lower Mach numbers did not produce any directed beams that one could observe with the continuous schlieren system, because the radiation was weaker and not strongly directional. For the same reasons, with a turbulent boundary layer ahead of the cavity it was hard to obtain any continuous-light pictures of the beam even for small gaps at high-subsonic Mach numbers.

Although it is not proposed to discuss in this report the mechanism of the sound production, it may be of interest to note that vortex motion in the gap may be an essential feature of the problem. It was observed that for some combinations of Mach number and gap breadth the phenomena in the gap were unstable in the sense that two intermittent frequencies could be measured. These frequencies were related as a fundamental and its harmonic (see the section "Frequency Measurements"). In general, the processes in the gap appeared much more violent in the case of turbulent boundary layer than in the laminar case.

The above description applies to observations on the variable gap in which the depth was fixed for all gap sizes. Experiments done on gaps of 0.05-inch depth showed similar acoustic radiations. No sound emission was observed for a gap width less than 0.05 inch. In figure 8 emission at  $M_\infty = 0.854$  from a gap 0.05 inch by 0.1 inch is shown.

In order to determine if any sound production results for flow over large cavities with thick turbulent boundary layers ahead, gaps 0.5 inch deep and 0.25 inch to 2 inches wide in the top wall of the tunnel were studied at Mach numbers from 0.2 to 1.4. No frequency measurements were made. Without entering into any details of these observations, it is sufficient at present to note that acoustic radiation did result from such flows. The radiation from a gap 0.5 inch deep and 0.25 inch broad at a Mach number of 1.3 is shown in figure 9.

#### FREQUENCY MEASUREMENTS

The frequencies were measured in the gap by using a hot-wire at constant current and examining the output on two wave analyzers, one for the ultrasonic range and the other for the audio range.

The wave analyzer was connected across the signal to be measured and was tuned over its entire frequency range. The frequency components of the input signal were determined by noting the peaks in the output of the analyzer. Typical plots of the analyzer output for the gap widths 0.095 inch and 0.31 inch and at a Mach number of 0.81 are shown in figures 10(a) and 10(b).

Measurements of frequency were made by varying the gap breadth gradually while maintaining the flow at a constant free-stream Mach number  $M_\infty$  and at a constant stagnation temperature  $T_0$ . The frequency  $f$  at a given value of  $M_\infty$  and  $T_0$  was found to be inversely proportional to the gap breadth  $b$ :

$$f = \alpha \frac{1}{b} \quad (1)$$

The constant of proportionality  $\alpha$  was different for laminar and turbulent layers and was usually lower for turbulent layers (cf. figs. 6 and 11).

#### Laminar Case

As an example of the measured frequencies in the laminar case, a plot of  $f$  against  $1/b$  at a Mach number of 0.815 and a stagnation temperature of  $116.8^\circ\text{F}$  is presented in figure 12. The dominant frequency and the first harmonic are shown. The harmonic frequency is twice the corresponding dominant frequency. The range of gap breadths covered for the measurements was from 0.1 inch to 0.5 inch. It may be noted that most of the frequencies measured for this case were in the ultrasonic range.

The results of the frequency measurements at different Mach numbers for the laminar case are shown in figure 6. Only the dominant frequencies are included. The solid portions of the lines indicate the range of gap widths covered for the measurements. Except for gap widths around the minimum (when acoustic radiation begins) and around 0.5 inch, the dominant and its harmonic were generally the only frequencies that were observed. For breadths around the minimum an additional frequency of about half the dominant was usually observed. For breadths near 0.5 inch and above, more than one higher harmonic could be noted.

Measurements in supersonic flow showed similar linear relationships between  $f$  and  $1/b$ . Figure 13 shows the results of measurements at  $M_\infty = 1.5$ .

Some additional, independent measurements in the supersonic case are available from the work of Vrebalovich (ref. 1), who used an alternating-current glow anemometer to measure the frequency of the sound emitted in supersonic flow from a cavity cut into a wedge. Figure 14, which is reproduced from this reference, shows these measurements.

#### Turbulent Case

Measurements of frequency with turbulent boundary layer were made for Mach numbers of 0.8, 0.75, 0.7, and 0.65 only. The results of these measurements differed from those of the laminar case mainly in one respect. While in the laminar case only a single dominant frequency was observed at a given gap width and Mach number, in the turbulent case two frequencies of nearly equal strength were recorded. The higher of these frequencies, which shall be referred to as the "high," was nearly twice the other, which shall be referred to as the "low." When at any particular setting of  $b$  and  $M_\infty$  frequencies besides these dominants were

measured, it was found that all the observed frequencies were usually harmonically related to the low as fundamental. The variation of high and low frequencies with  $1/b$  at different Mach numbers is shown in figure 11. Comparing this plot with that of figure 6, it may be noted that the high frequencies for the turbulent-boundary-layer case are of the same order as the dominant frequencies for the laminar case.

For some combinations of  $U_\infty$  and  $b$ , the phenomena in the gap were unstable and the radiation was intermittent. As an example, intermittency observed for  $b = 0.5$  inch at  $M_\infty = 0.75$  and  $T_0 = 116.8^\circ \text{F}$  is shown in figure 15, which is a plot of  $f$  against  $1/b$  for  $M_\infty = 0.75$ . The dominant high frequency component B (equal to 13.9 kilocycles) was present when the components A and C (equal to 6.6 and 19.2 kilocycles, respectively) were absent, and vice versa. When A and C were present a note could be heard (A is in the audible range) which momentarily disappeared when component B was present. A slight change in temperature  $T_0$  or the gap width  $b$  would cause this instability to disappear. This behavior, which apparently results from the coexistence of two stable states in the gap, was observed to be a typical feature of flow past gaps of breadths around 0.5 inch and greater with a turbulent boundary layer.

#### Nondimensional Frequency

Obviously one would like to form a dimensionless frequency or Strouhal number. The measurements have shown that the frequency  $f$  is related to  $b$ , the breadth of the cavity. To form a Strouhal number a characteristic velocity has to be chosen. If one uses  $U_\infty$ , the free-stream velocity, one has

$$S = f \frac{b}{U_\infty} \quad (2)$$

It has been seen that, for a given free-stream Mach number  $M_\infty$  and stagnation temperature  $T_0$ ,

$$fb = \text{Constant} = \alpha \quad (3)$$

The constant  $\alpha$  is then a function of  $M_\infty$  and possibly  $T_0$ . The dependence of  $\alpha$  on  $T_0$  was not fully examined, though in the range of the tests made it was found to be reasonably constant for small changes in  $T_0$ . Thus,

$$S = \alpha \frac{1}{U_\infty} = \alpha \frac{1}{a_0} \frac{1}{U_\infty/a_0} \quad (4)$$

where  $\alpha$  is the slope of the line  $f$  versus  $1/b$  and is, therefore, known from figures 6 and 11. Furthermore, for a given value of  $M_\infty$ ,  $U_\infty/a_0$  is known from isentropic-flow relations.

In figure 16  $S$  is plotted against  $M_\infty$  for both laminar- and turbulent-boundary-layer cases. The dependence of  $S$  on the gap depth, particularly as it is related to the boundary layer, has not yet been investigated.

For supersonic flow the nondimensional frequency is defined with respect to the flow velocity  $U_1$  immediately ahead of the upstream edge of the gap. Thus, in supersonic flow,

$$S = \frac{\alpha}{U_1} = \frac{\alpha}{a_0} \frac{1}{\left(\frac{a_\infty}{a_0}\right)\left(\frac{a_1}{a_\infty}\right)M_1} \quad (5)$$

The value of  $S$  for the Mach number  $M_\infty = 1.5$  is included in figure 16.

#### Measurement of Local Speed of Sound

The experimental method of obtaining the local speed of sound in a fluid medium by means of sonic waves is based on the principle that the propagation velocity normal to the wave fronts is equal to the speed of sound  $a$ . The propagation velocity is related to the frequency  $f$  and the wavelength  $\lambda$  of the sound by

$$a = f\lambda \quad (6)$$

Thus, if sound waves of known frequency are produced in the medium and their wavelengths are measured by means of instantaneous schlieren pictures, the sound velocity is easily determined. It appears therefore that the acoustic radiation from a cavity in high-speed flow could be used for such determinations. The frequency of the radiation is known by measurement while the wavelength can be determined in the following way:

Assuming that the acoustic field, as observed on the instantaneous schlieren pictures, is similar to that produced by a two-dimensional stationary source radiating into a moving stream, a simple geometric construction will enable one to estimate from such pictures the wavelength of the emitted sound. This method is illustrated in figure 17. Choosing a point  $P$  on any wave front, one knows that this point propagates with a velocity vector  $\vec{V}$  given by

$$\vec{V} = \vec{a} + \vec{U} \quad (7)$$

where  $\vec{a}$  is the local velocity of sound directed normally to the wave front at the point considered and  $\vec{U}$  is the velocity of the flow at P. Taking  $\vec{U} = \vec{U}_\infty$ , the free-stream velocity, and dividing equation (7) by  $|\vec{a}|$ , the local speed of sound, one obtains

$$\frac{\vec{V}}{|\vec{a}|} = \vec{n} + M_\infty \vec{u}_1 \quad (7a)$$

where  $\vec{n}$  is a unit vector in the direction of the normal to the wave front at P and  $\vec{u}_1$  is a unit vector in the direction of the free-stream velocity. Hence, it is simple to construct the velocity vector  $\vec{V}$  at the point P, knowing only the Mach number  $M_\infty$  and choosing any scale for the local speed of sound  $|\vec{a}|$ . The point  $P_1$  where the relative velocity vector  $\vec{V}$  intersects the next wave front then corresponds to P. A line drawn from  $P_1$  parallel to  $\vec{u}_1$  and intersecting vector  $\vec{n}$  from P determines to scale the wavelength  $\lambda$  of the waves, as shown in the figure. The absolute value of  $\lambda$  is obtained from the scale determined by the gap breadth.

For purposes of illustration the local speed of sound is computed from the measured values of frequency and wavelength of the radiation field for a gap 0.2 inch wide by 0.1 inch deep in a flow of  $M_\infty = 0.815$  and  $T_0 = 117^\circ \text{ F}$ . The measured wavelength is 0.323 inch and the measured frequency is 39 kilocycles. These give a local speed of sound equal to 1,050 feet per second. Within the limits of accuracy of measuring the frequency and the wavelength, this value compares well with the speed of sound computed in the usual way from the stagnation temperature and the free-stream Mach number, which in this case is 1,100 feet per second.

#### INTENSITY OF ACOUSTIC RADIATION

The intensity of radiation is the rate at which energy is transmitted across a unit area of a plane parallel to the wave front. For a simple harmonic wave of frequency  $f$  the intensity  $I$  is given by the relation

$$I = \frac{1}{2} \frac{p^2}{\rho_e a} \quad (8a)$$

or

$$I = \frac{1}{2} \rho_e a^3 (\delta^*)^2 \quad (8b)$$

where  $a$  is the local speed of sound;  $P$  and  $\delta^*$  are the maximum amplitudes of the pressure and condensation waves, respectively;  $\rho_e$  is the equilibrium value of the local density of the medium; and  $I$  is expressed in ergs per square centimeter per second.

In the decibel scale the intensity is given by its level relative to the reference level  $10^{-9}$  erg per square centimeter per second. Thus,

$$I_{db} = 10 \log_{10} \frac{I}{I_{ref}}$$

where  $I_{db}$  is the intensity in decibels and  $I_{ref}$  is the reference intensity  $10^{-9}$  erg per square centimeter per second. Hence,

$$I_{db} = 90 + 10 \log_{10} I \quad (9)$$

An optical interferometer of the Mach-Zehnder type is very suitable to measure intense sound fields. One measures the maximum amplitude of the condensation at any desired point in the acoustic field by means of "no-flow" and "with-flow" finite-fringe interferograms (of very short duration) of the field. The fringe shift and the "condensation" are related by:

$$\frac{\Delta x}{x} = \frac{l}{\lambda_v} k \Delta \phi$$

or

$$\delta = \frac{\rho - \rho_e}{\rho_e} = \frac{\Delta \phi}{\rho_e} = \frac{\Delta x}{x} \frac{\lambda_v}{l} \frac{1}{k \rho_e} \quad (10)$$

where

$\rho$	instantaneous local density
$\Delta x$	fringe shift (measured as distance)
$x$	fringe spacing, distance between two consecutive fringes
$\lambda_v$	wave length (in vacuum) of light used, 5,170 Å (magnesium line)
$k$	Gladstone-Dale constant (table 349, ref. 2), $0.0017 \text{ cm}^3/\text{g}$
$l$	span of model, 3.996 in.

Thus an instantaneous with-flow interferogram of the field is a measure of the wave form of the condensation and one can simply obtain the maximum amplitude of the condensation by measuring the corresponding fringe shift. Thus,

$$\delta^* = \left( \frac{\Delta x}{x} \right)_m \frac{\lambda_v}{l} \frac{1}{k \rho_e} \quad (11)$$

where  $\left( \frac{\Delta x}{x} \right)_m$  is the maximum amplitude of the fringe shift.

From relations (8b) and (11) one obtains

$$I = \frac{1}{2} \rho_e a^3 \left[ \left( \frac{\Delta x}{x} \right)_m \frac{\lambda_v}{l} \frac{1}{k \rho_e} \right]^2$$

which may be rewritten as

$$I = \frac{1}{2} \left( \frac{a}{a_0} \right)^3 a_0^3 \frac{1}{\left( \frac{\rho_e}{\rho_0} \right) \rho_0} \left( \frac{\lambda_v}{l} \right)^2 \frac{1}{k^2} \left( \frac{\Delta x}{x} \right)_m^2 \quad (12)$$

if  $a$  and  $\rho_e$  are expressed in terms of the stagnation conditions  $a_0$  and  $\rho_0$ , respectively.

This relation is the basis for the evaluation of the intensity of the acoustic radiation. At a Mach number of 0.7 or 0.8 and for

$T_0 = 110^\circ \text{ F}$ , a unit fringe shift (i.e.,  $\left( \frac{\Delta x}{x} \right)_m = 1$ ) corresponds to an intensity of 163 decibels. Fringe shifts equal to and greater than 1 were observed for these radiations, indicating that the acoustic fields were very intense.

A few typical finite-fringe interferograms of the acoustic field are presented in figure 18. It may be observed that the intensity of radiation from a gap of 0.3-inch breadth at  $M_\infty = 0.82$  is greater with laminar boundary layer than with turbulent flow. Further, the intensity for a gap 0.2 inch wide at  $M_\infty = 0.7$  is comparable with that for a gap 0.3 inch wide at  $M_\infty = 0.82$ .

Figure 19 shows infinite-fringe interferograms of the radiation in laminar flow from a gap 0.3 inch wide for  $M_\infty = 0.816$ . These pictures were taken under identical free-stream conditions. They are indicative of the changes taking place within the gap and in the field. Consequently, it should be fruitful to undertake studies of the mechanism of the acoustic radiation by means of infinite-fringe interferograms.

## CONCLUDING REMARKS

Two-dimensional rectangular cavities cut into aerodynamic surfaces are found to emit intense acoustic radiation in high-speed flow. The acoustic fields due to different gaps in varying flow conditions were studied by means of schlieren, hot-wire, and optical interferometric techniques.

It was shown that high-frequency radiation, strong and directional, resulted from small gaps of 0.1- to 0.2-inch width and 0.1-inch depth in laminar flow at Mach numbers of 0.8.

At a particular Mach number the frequency, as measured in the gap by a hot-wire, was shown to be inversely proportional to gap breadth in both laminar and turbulent flows. The dependence on depth has not yet been investigated.

It was indicated that the local speed of sound in high-speed flow could be computed from the measured frequency and wavelength of the radiation from a cavity. A method of obtaining the wavelength from the spark schlieren photographs was given.

The use of an optical interferometer of the Mach-Zehnder type to measure the intensity of the radiation was demonstrated.

Important practical and fundamental applications of this new phenomenon are possible. Studies of the mechanism of the radiation may lead to a better understanding of the problems of buffeting in cavities, such as bomb bays and cockpits. The production of sound from these cavities is a typical example of the conversion of aerodynamic shear energy into acoustic energy. Small cavities should prove very successful as efficient and cheap sources of ultrasonic sound for measurement of local fluid properties in high-speed flow. Further, known disturbances, such as those resulting from these gaps, could be used for studies of laminar-boundary-layer stability and for the production of turbulence by interaction of sound with shock waves.

California Institute of Technology,  
Pasadena, Calif., September 20, 1954.

## REFERENCES

1. Vrebalovich, Thomas: The Development of Direct and Alternating Glow Discharge Anemometers for Study of Turbulence Phenomena in Supersonic Flow. Ph. D. Thesis, C.I.T., 1954.
2. Fowle, Frederick E.: Smithsonian Physical Tables. Seventh rev. ed., Smithsonian Institution, 1920, p. 293.

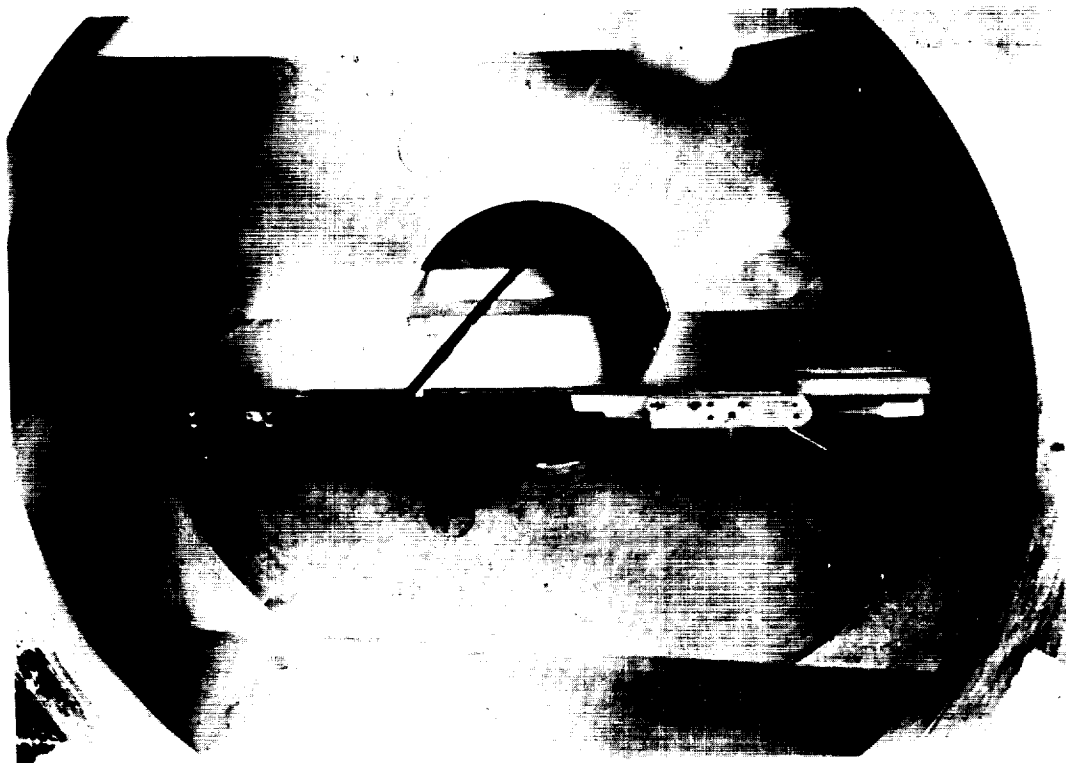


Figure 1.- Variable-gap model in test section. L-87929

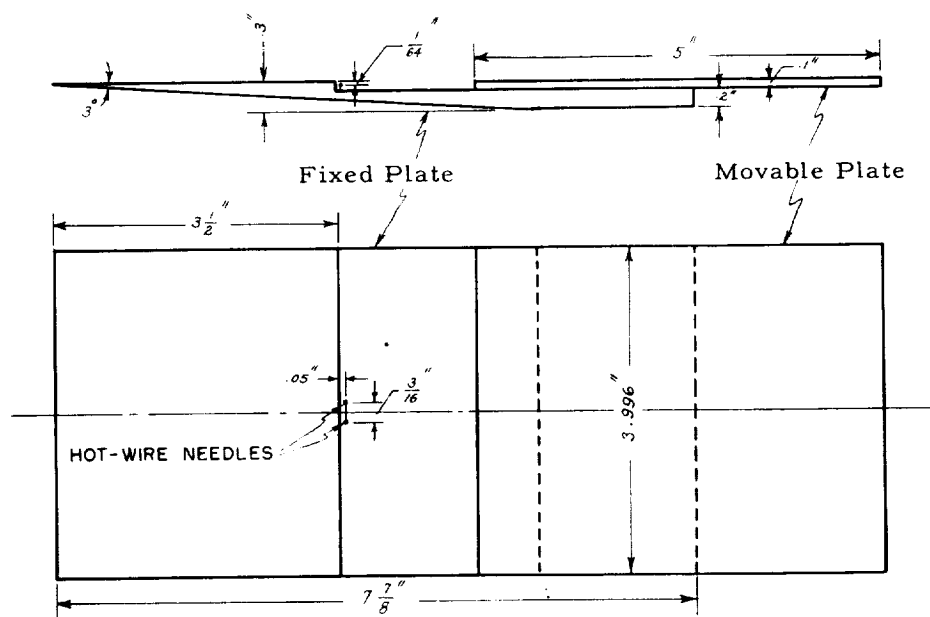
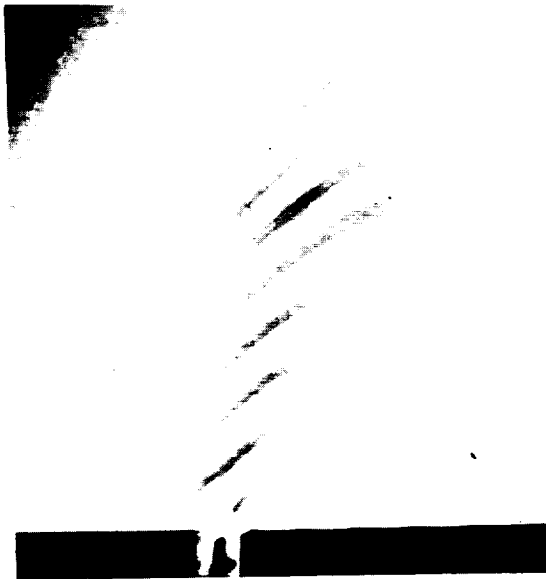


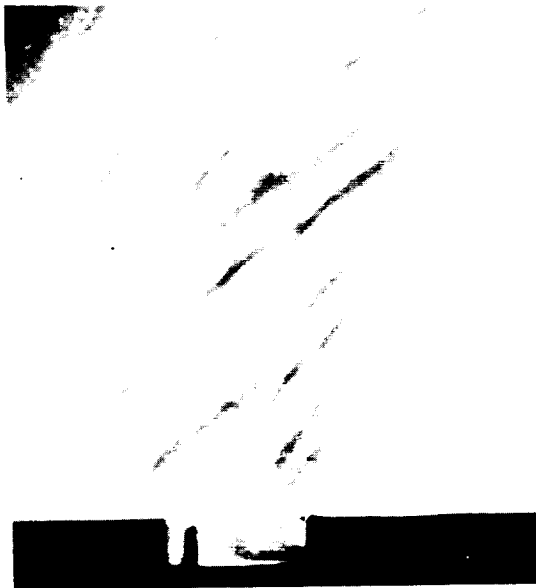
Figure 2.- Dimensional sketch of model.



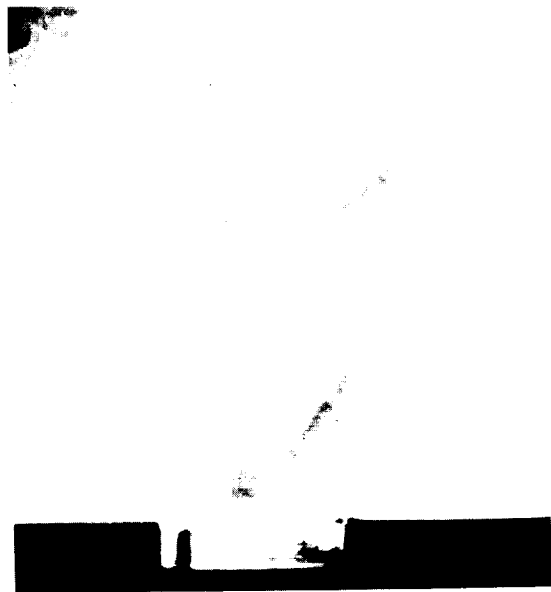
(a) Gap with  $d = 0.1$  inch  
and  $b = 0.1$  inch. Knife  
edge horizontal.



(b) Gap with  $d = 0.1$  inch  
and  $b = 0.2$  inch. Knife  
edge vertical.



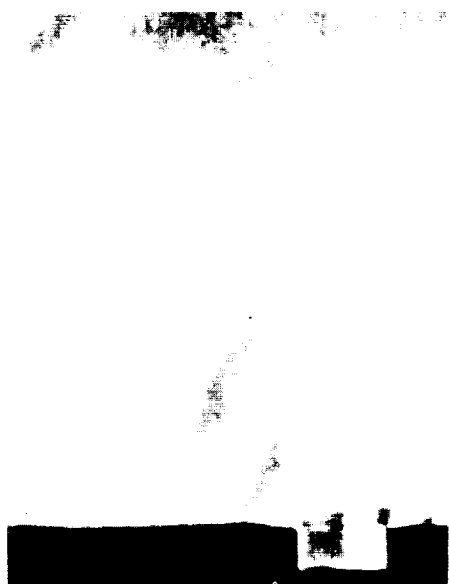
(c) Gap with  $d = 0.1$  inch  
and  $b = 0.3$  inch. Knife  
edge horizontal.



(d) Gap with  $d = 0.1$  inch  
and  $b = 0.4$  inch. Knife  
edge horizontal.

L-87930

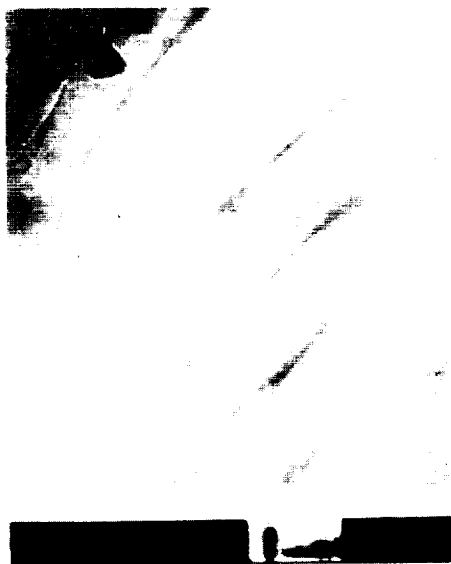
Figure 3.- Sound emission for increasing gap breadths with laminar bound-  
ary layer.  $M_\infty = 0.815$ ;  $T_0 = 116.8^\circ \text{ F}$ .



(a)  $M_\infty = 0.5$ ;  $T_0 = 105^\circ \text{ F.}$   
Knife edge vertical.



(b)  $M_\infty = 0.64$ ;  $T_0 = 116.8^\circ \text{ F.}$   
Knife edge vertical.



(c)  $M_\infty = 0.695$ ;  $T_0 = 116.8^\circ \text{ F.}$   
Knife edge horizontal.



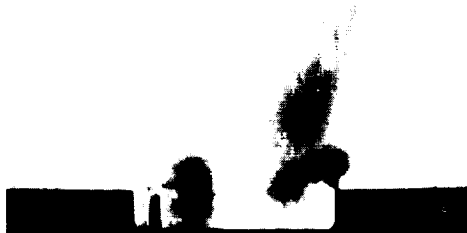
(d)  $M_\infty = 1.384$ ;  $T_0 = 116.8^\circ \text{ F.}$   
Knife edge vertical.

Figure 4.- Sound emission for gap 0.1 inch deep and 0.2 inch wide with laminar boundary layer at different Mach numbers.



(a) Gap with  $d = 0.1$  inch  
and  $b = 0.2$  inch. Knife  
edge horizontal.

(b) Gap with  $d = 0.1$  inch  
and  $b = 0.3$  inch. Knife  
edge vertical.



L-87932

(c) Gap with  $d = 0.1$  inch  
and  $b = 0.5$  inch. Knife  
edge vertical.

Figure 5.- Sound emission for increasing gap breadths with turbulent  
boundary layer.  $M_\infty = 0.804$ ;  $T_0 = 116.8^\circ \text{ F}$ .

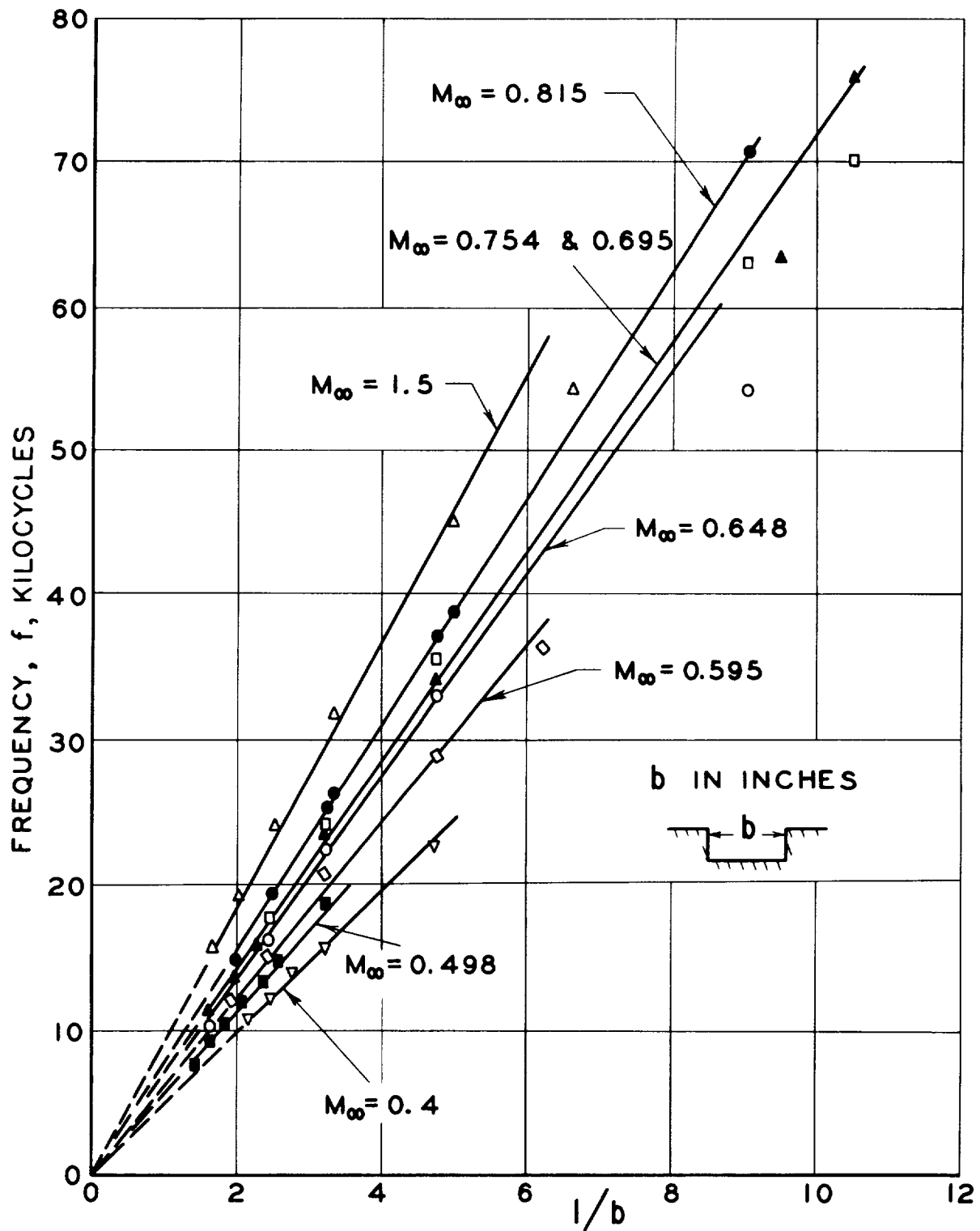


Figure 6.- Results of frequency measurements for laminar case at different Mach numbers.

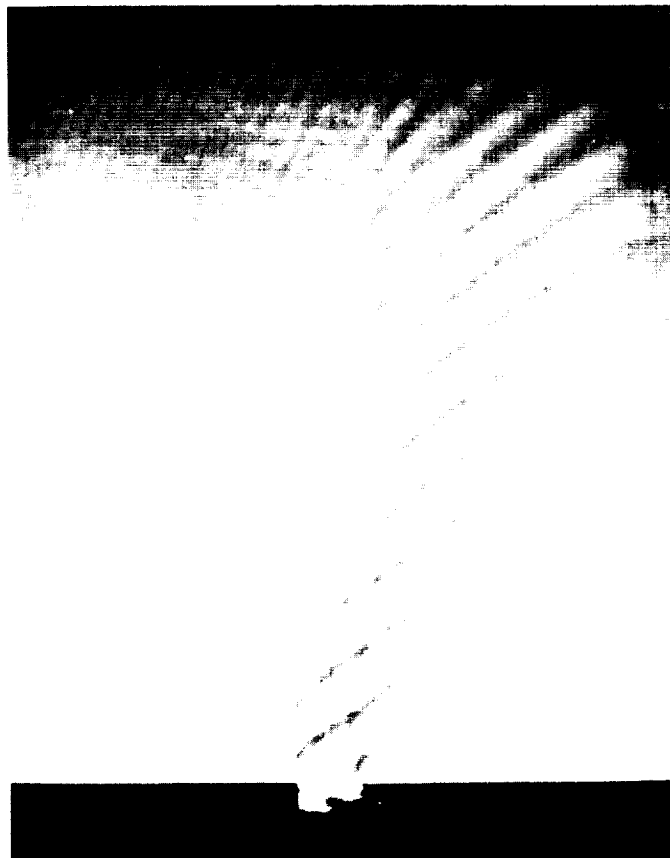


(a)  $d = 0.1$  inch;  $b = 0.1$  inch.



L-87933  
(b)  $d = 0.1$  inch;  $b = 0.2$  inch.

Figure 7.- Continuous-light schlieren photographs of sound emission for gap breadths of 0.1 and 0.2 inch with laminar boundary layer.  
 $M_{\infty} = 0.803$ ;  $T_0 = 116.8^{\circ}$  F.



L-87934

Figure 8.- Sound emission for gap 0.05 inch deep and 0.1 inch broad with laminar boundary layer.  $M_\infty = 0.854$ ;  $T_o = 116.8^\circ \text{ F}$ .



L-87935

Figure 9.- Sound emission for gap 0.5 inch deep and 0.25 inch broad  
on tunnel top block with turbulent boundary layer.  $M_{\infty} = 1.3$ ;  
 $T_o = 116.8^{\circ} \text{ F.}$

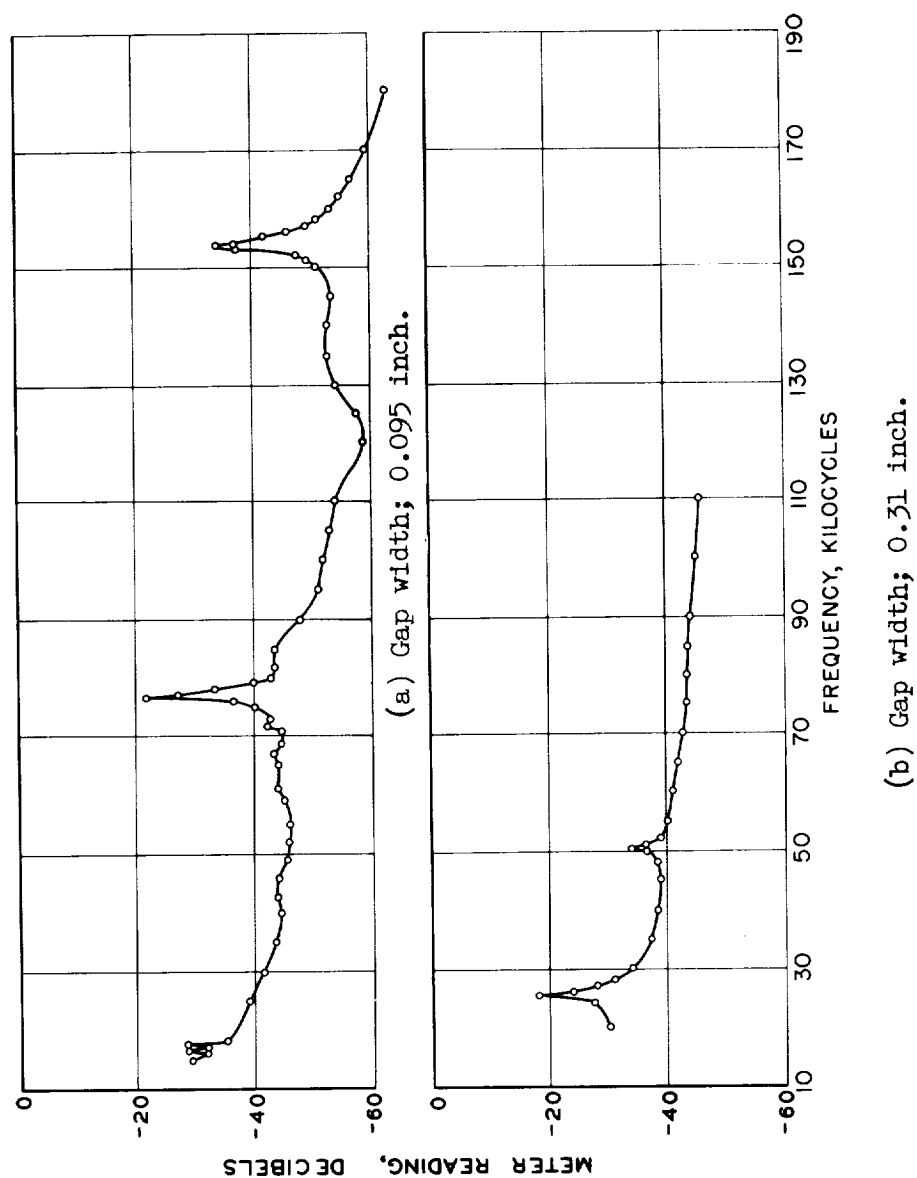


Figure 10.- Typical frequency distribution of analyzer-meter readings.  
 $M_{\infty} = 0.81$ ; laminar flow.

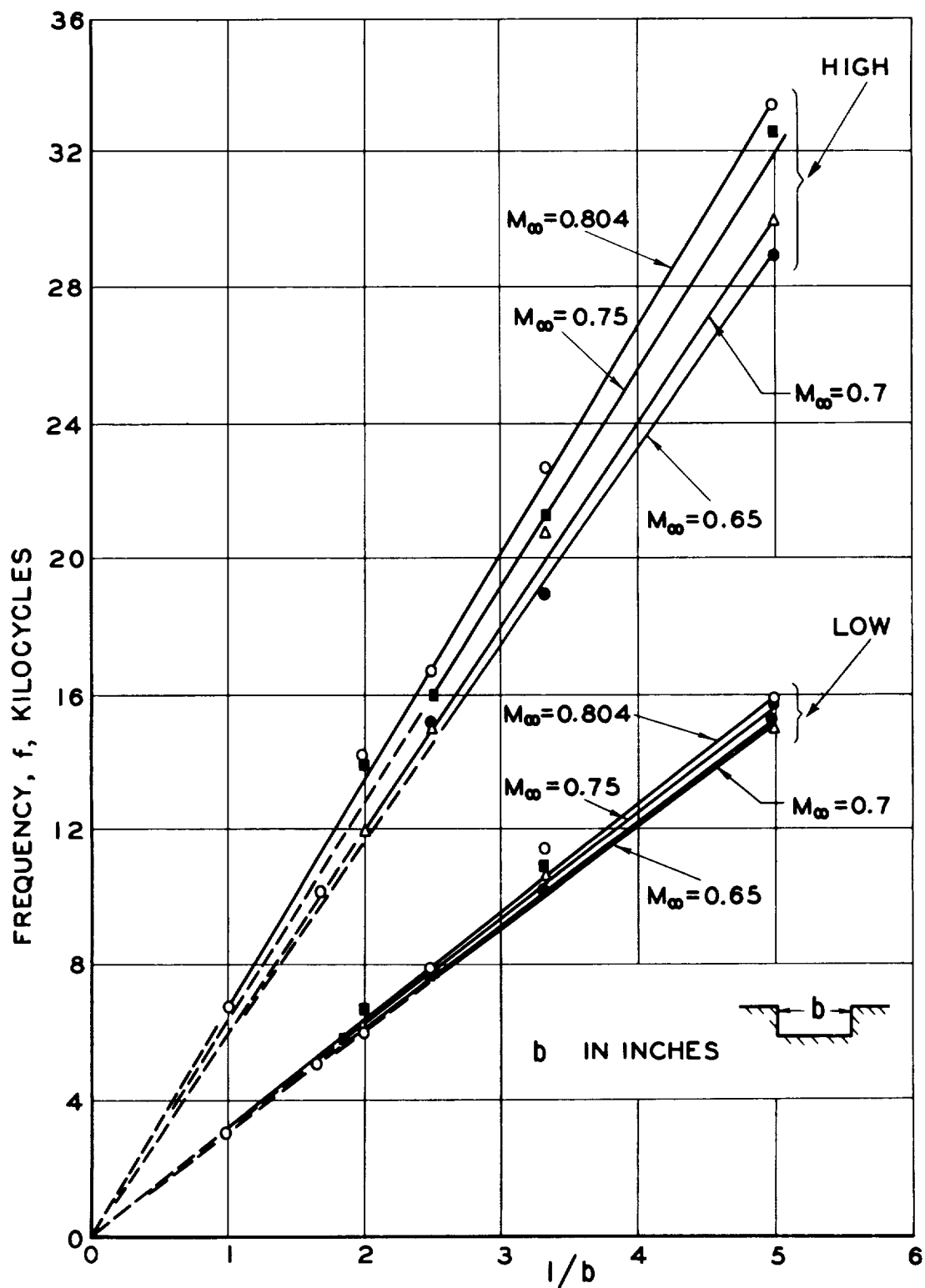


Figure 11.- Results of frequency measurements for turbulent case at different Mach numbers.  $T_o = 116.8^\circ \text{ F.}$

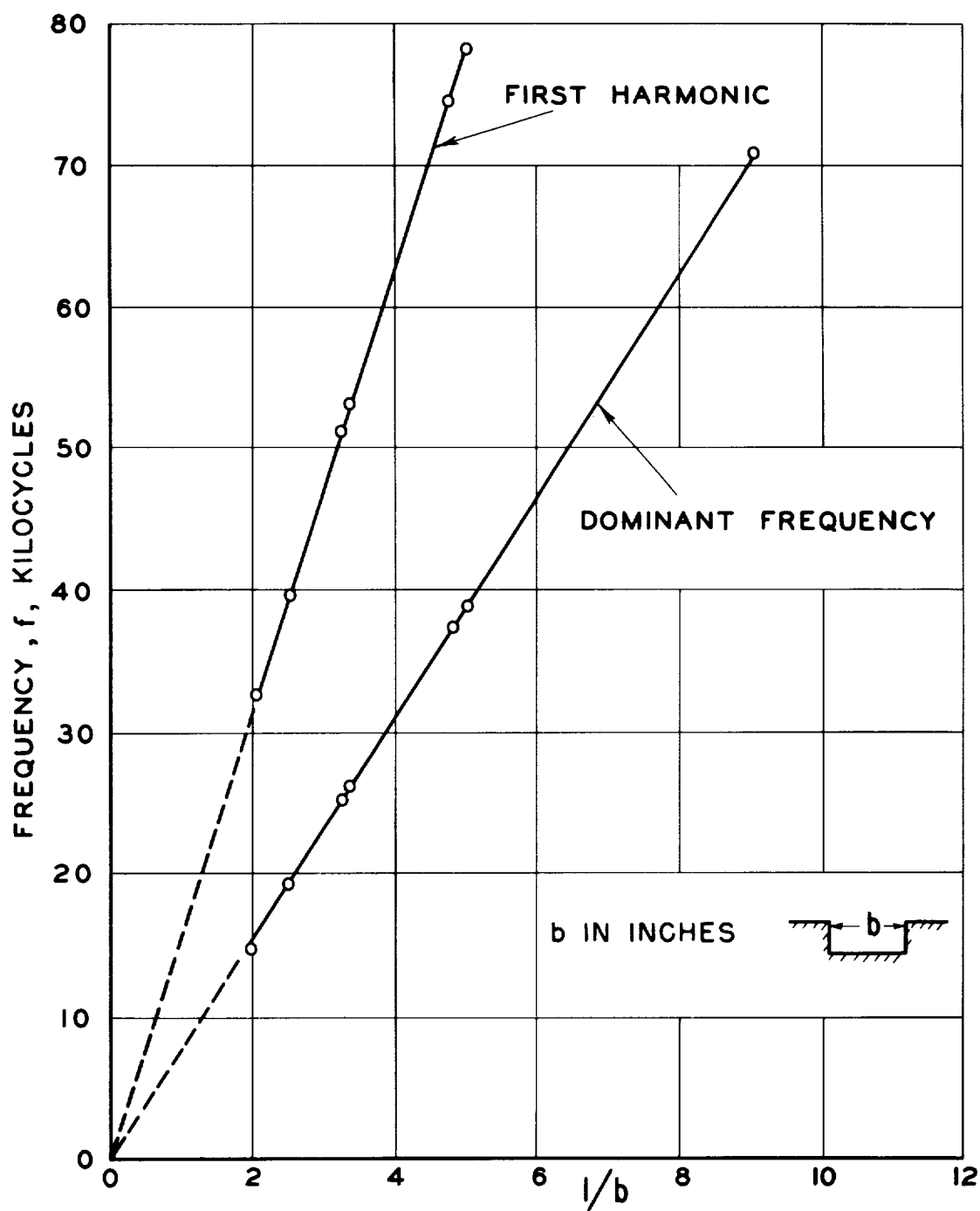


Figure 12.- Results of frequency measurements for laminar case for range of gap breadths from 0.1 to 0.5 inch.  $M_\infty = 0.815$ ;  $T_0 = 116.8^\circ \text{F}$ .

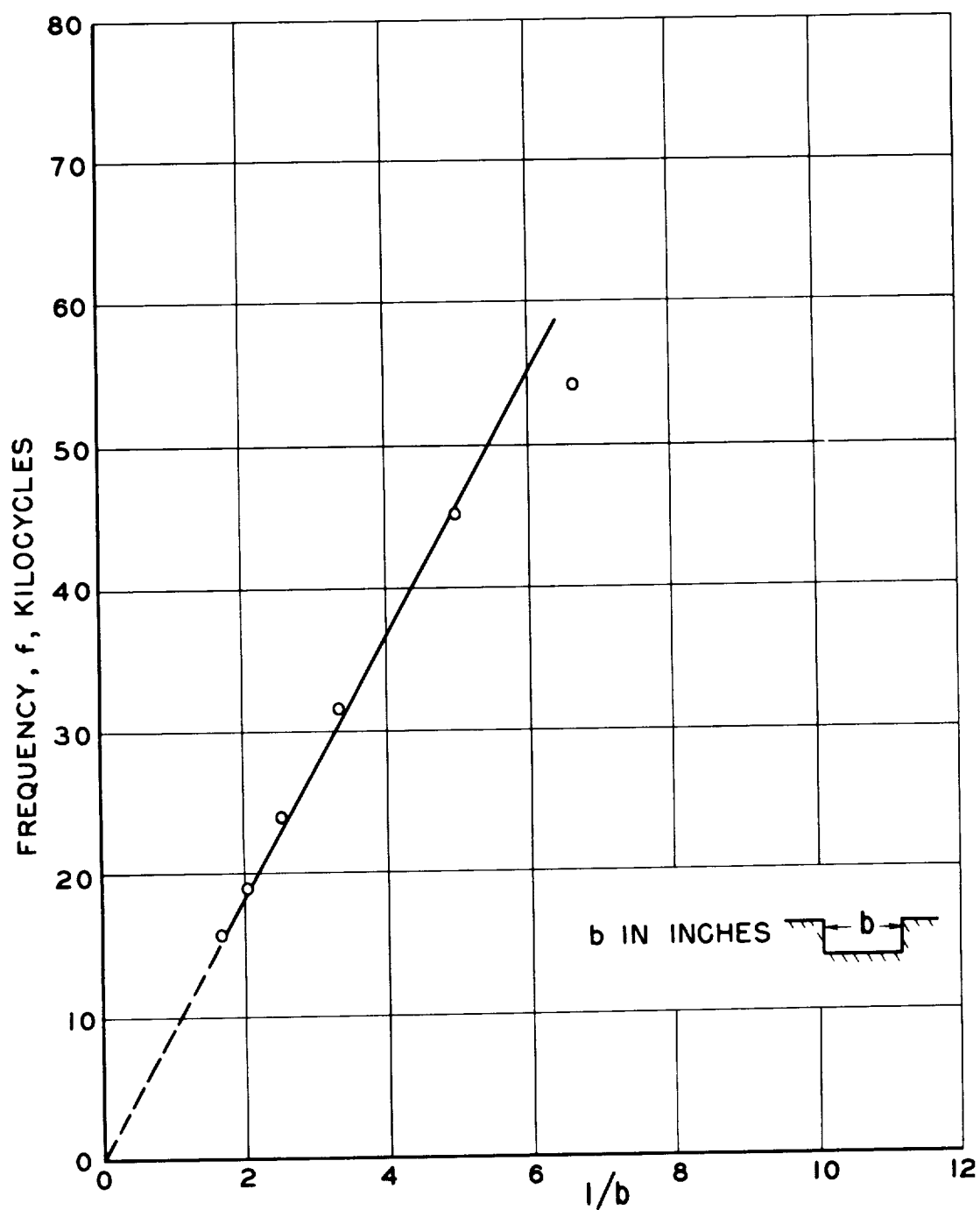
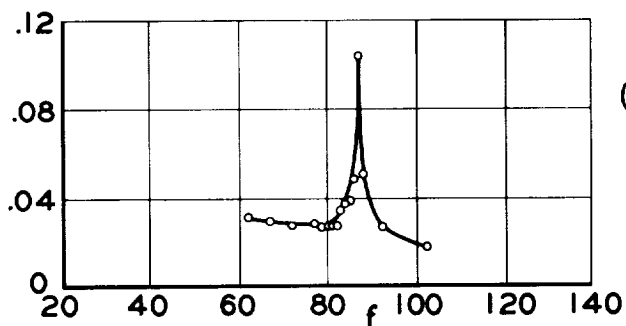
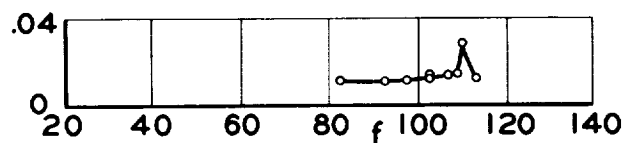


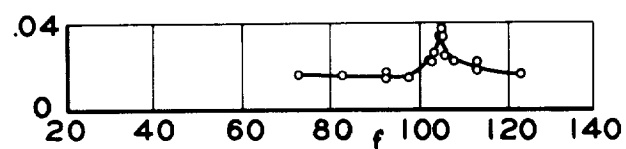
Figure 13.- Results of frequency measurements for laminar case in supersonic flow.  $M_\infty = 1.5$ ;  $T_0 = 123.2^\circ \text{F}$ .



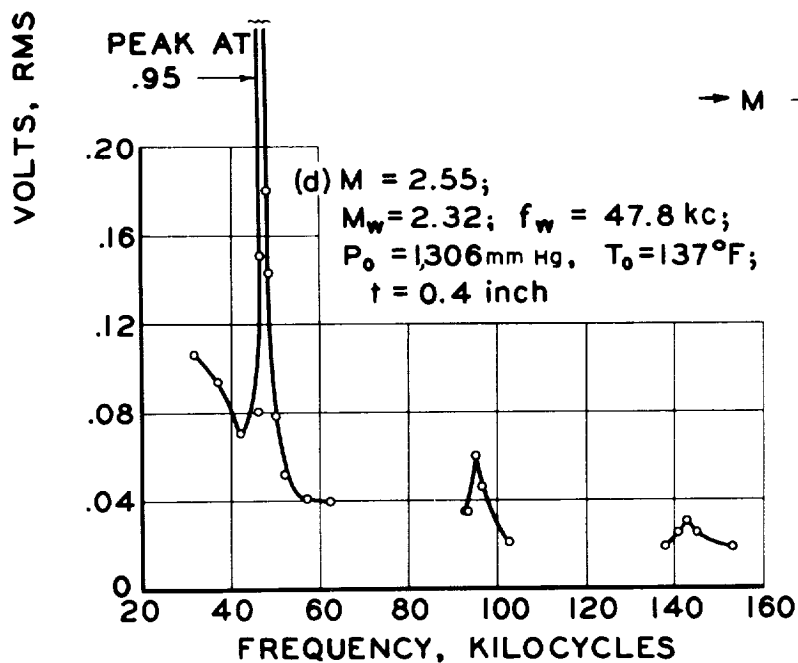
(a)  $M = 1.97$ ;  
 $M_w = 1.80$ ;  $f_w = 87.2$  kc;  
 $P_o = 1,391$  mm Hg;  $T_o = 131^\circ\text{F}$ ;  
 $t = 0.2$  inch



(b)  $M = 2.55$ ;  
 $M_w = 2.32$ ;  $f_w = 109.7$  kc;  
 $P_o = 1,302$  mm Hg;  $T_o = 134^\circ\text{F}$ ;  
 current, 14 ma;  
 $t = 0.2$  inch



(c)  $M = 2.55$ ;  
 $M_w = 2.32$ ;  $f_w = 104.8$  kc;  
 $P_o = 726$  mm Hg;  $T_o = 108^\circ\text{F}$ ;  
 current, 10 ma;  
 $t = 0.2$  inch



(d)  $M = 2.55$ ;  
 $M_w = 2.32$ ;  $f_w = 47.8$  kc;  
 $P_o = 1,306$  mm Hg;  $T_o = 137^\circ\text{F}$ ;  
 $t = 0.4$  inch

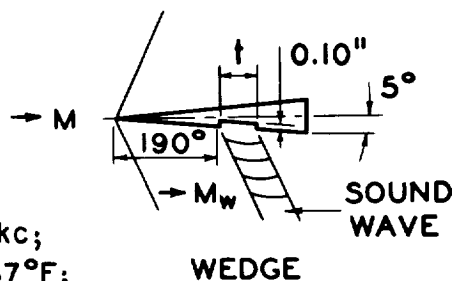


Figure 14.- Disturbance frequency induced by a slot in a wedge in supersonic flow. (From ref. 1.)

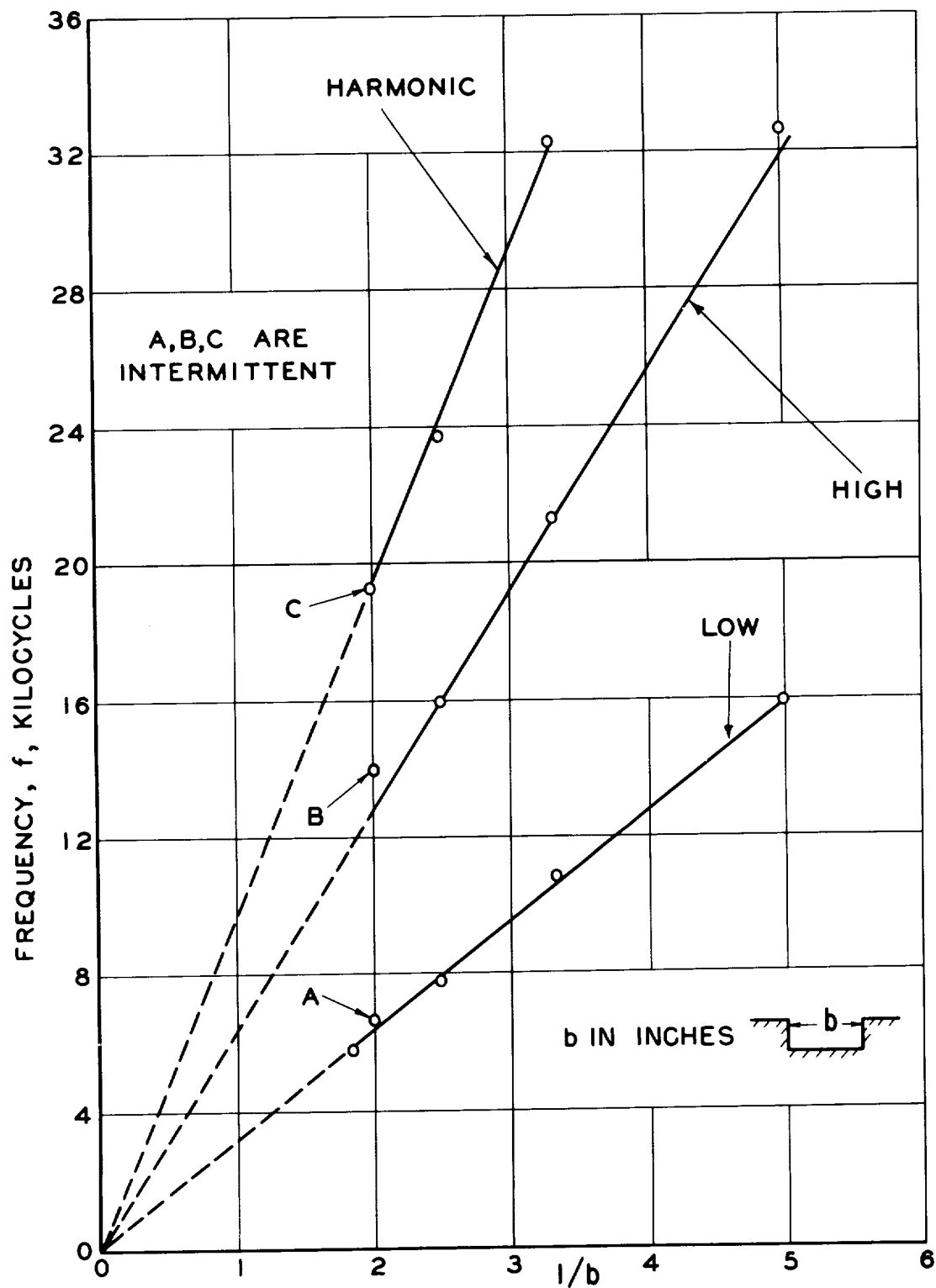


Figure 15.- Results of frequency measurements for turbulent case showing intermittency observed for  $b = 0.5$  inch.  $M_\infty = 0.75$ ;  $T_0 = 116.8^\circ \text{F}$ .

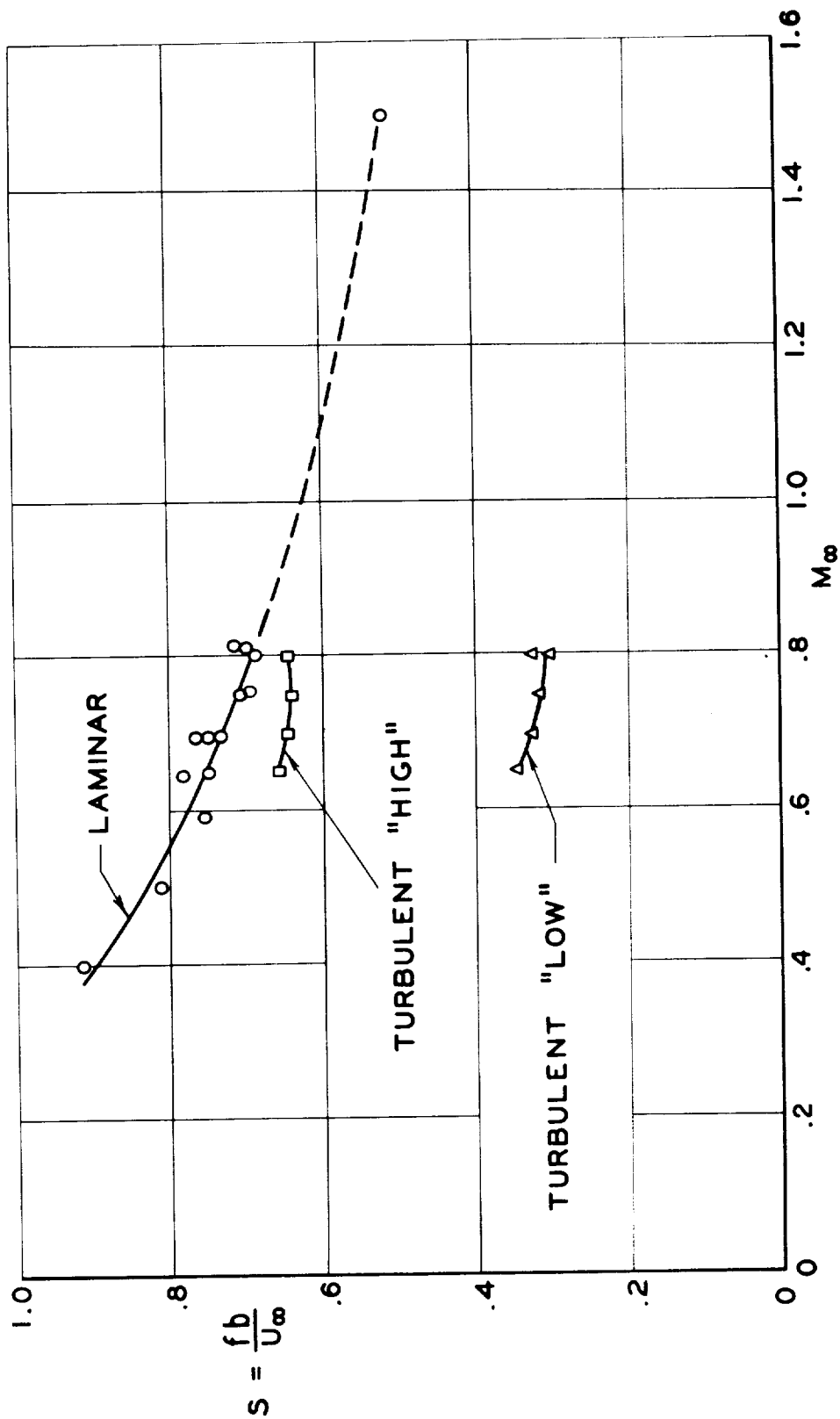


Figure 16.- Nondimensional frequency.

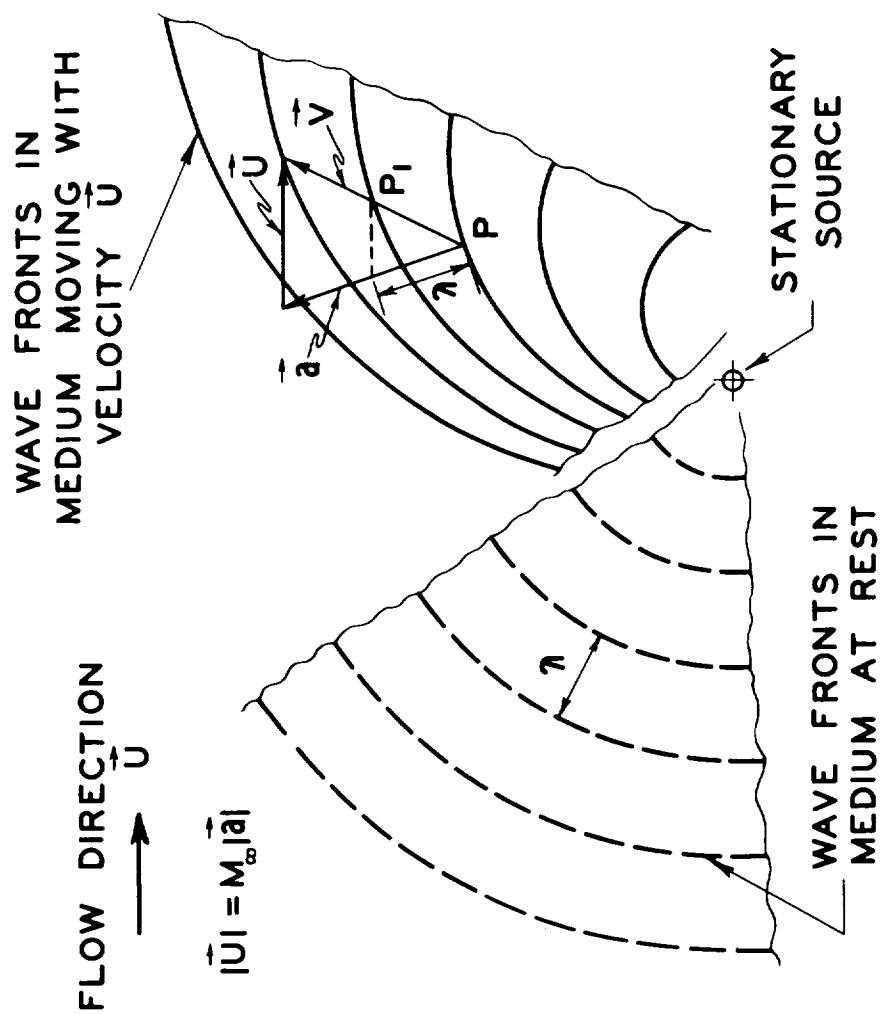
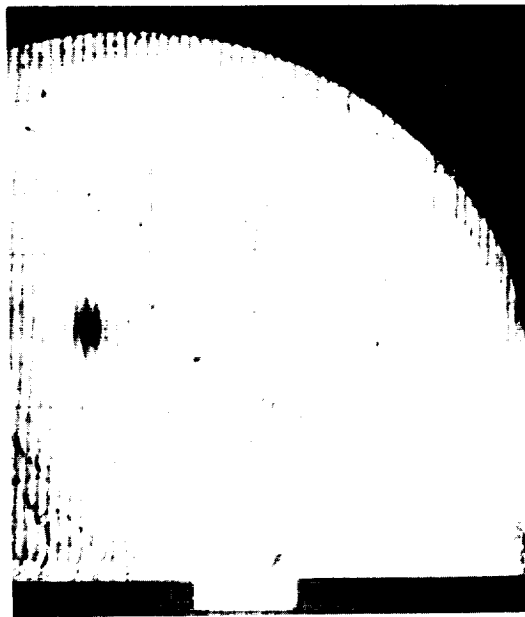


Figure 17.- Acoustic field due to a stationary source radiating into a moving stream.



(a)  $M_\infty = 0.82$ ;  $b = 0.3$  inch;  
laminar layer.



(b)  $M_\infty = 0.82$ ;  $b = 0.3$  inch;  
turbulent layer.



(c)  $M_\infty = 0.7$ ;  $b = 0.2$  inch;  
laminar layer.

L-87936

Figure 18.- Finite-fringe interferograms.



(a)



(b)



(c)

Figure 19.- Infinite-fringe interferograms.  $M_\infty = 0.816$ ;  $b = 0.3$  inch; laminar layer.

